Solid solution softening at room temperature and hardening at elevated temperatures: a case by minor Mn addition in a

Materials Research Express

PAPER • **OPEN ACCESS**

Solid solution softening at room temperature and hardening at elevated temperatures: a case by minor Mn addition in a $(HfNbTi)_{85}Mo_{15}$ refractory high entropy alloy

To cite this article: Xiaolong Li *et al* 2023 *Mater. Res. Express* **10** 116501

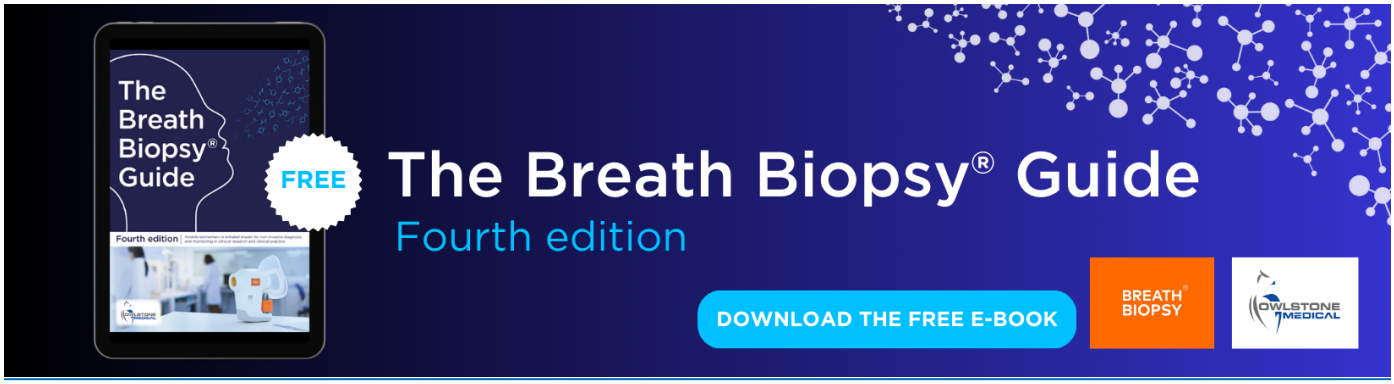

Materials Research Express

PAPER

Solid solution softening at room temperature and hardening at elevated temperatures: a case by minor Mn addition in a $(HfNbTi)_{85}Mo_{15}$ refractory high entropy alloy

Xiaolong Li[1], **Mao Ding**[2], **Qiang Hu**[3], **Zhiyuan Liu**[2], **Huahai Mao**[4] **and Sheng Guo**[1,*]

[1] Department of Industrial and Materials Science, Chalmers University of Technology, Gothenburg SE-41296, Sweden
[2] College of Mechatronics and Control Engineering, Shenzhen University, Shenzhen 518060, People's Republic of China
[3] Institute of Applied Physics, Jiangxi Academy of Sciences, Nanchang 330096, People's Republic of China
[4] Thermo-Calc Software AB, Råsundavägen 18A, SE-169 67 Stockholm, Sweden
[*] Author to whom any correspondence should be addressed.

E-mail: sheng.guo@chalmers.se

Keywords: refractory high entropy alloys, solid solution softening and hardening, solid solutions

OPEN ACCESS

RECEIVED
18 August 2023

REVISED
17 October 2023

ACCEPTED FOR PUBLICATION
24 October 2023

PUBLISHED
1 November 2023

Abstract

To address the conflict between room-temperature (RT) ductility and high-temperature (HT) strength in single phase bcc-structured refractory high entropy alloys, here we propose to use minor alloying to achieve solid solution softening at RT and simultaneously, solid solution hardening at HT. Our strategy was manifested by minor Mn additions in a RT brittle $(HfNbTi)_{85}Mo_{15}$ refractory high entropy alloy, where nominal Mn additions ranging from 2 at. % down to 0.03 at. % were seen to soften the base $(HfNbTi)_{85}Mo_{15}$ alloy at RT, while to harden the base alloy at the temperature range from 400 to 800 °C. The yield stress in all studied alloys showed a three-stage pattern, characterized by a temperature dependent stage at temperatures below 400 °C, followed by a temperature independent stage at intermediate temperatures ranging from 400 to 800 °C, and finally another temperature dependent stage at temperatures higher than 800 °C. The mechanisms for solid solution softening and solid solution hardening in single phase bcc-structured refractory high entropy alloys were discussed, together with their temperature dependence.

Introduction

Refractory high entropy alloys (RHEAs) [1, 2] with decent high temperature (HT) strength are promising candidates for next generation HT materials. Unfortunately, those RHEAs with decent HT strength generally suffer from room temperature (RT) brittleness [3]. To address the brittleness issue, one bottleneck facing the further development of RHEAs as novel HT materials, several ductilization strategies have been proposed, importantly including the valence electron concentration (VEC) approach [4, 5] and the metastability-engineering method [6]. Lowering VEC to achieve intrinsically ductile RHEAs typically requires alloying with Ti group metals (Ti, Zr, Hf) with relatively low melting points compared to other refractory elements, which is therefore difficult to achieve a decent HT strength. The metastability-engineering method is about destabilizing the body centered cubic (bcc) phase by decreasing the amount of bcc phase stabilizing elements or alternatively increasing the amount of the hexagonal close-packed (hcp) phase stabilizing elements, such as Ti group metals [6]. The above mentioned two ductilization strategies are essentially similar in that both involve heavy alloying or significantly increasing the amount of Ti group metals; consequently, both strategies ductilize RHEAs at the cost of compromised HT strength. Therefore, new strategies are urgently needed to improve the RT ductility of RHEAs, without sacrificing too much of their HT strength.

As noted by Senkov *et al* [7] it is relatively easy to identify alloys with good HT strength, but more difficult to locate alloys with both HT strength and RT ductility. Previously, more efforts were paid to develop intrinsically ductile RHEAs and then to strengthen them, and less to ductilize RHEAs that are strong but intrinsically brittle, mainly because there are many well established approaches for the former, but it is rather challenging for the

Table 1. Measured compositions of the tested alloys by EDS in atomic percent (at%). The Mn content was measured by ICP-OES, in weight percent (wt%).

Alloys	Ti	Hf	Nb	Mo	Mn
Base	32.2	27.6	25.8	14.3	
Mn2	31.0	27.9	26.2	14.9	0.0735
Mn1	30.7	27.4	26.9	15.1	0.067
Mn0.3	30.9	27.9	26.5	14.7	0.025
Mn0.1	30.7	27.7	26.8	14.8	0.0095
Mn0.03	31.4	27.6	26.2	14.7	0.0075

latter. However, strengthening ductile RHEAs so far shows little progress to break through the trade-off between HT strength and RT ductility, and one now really needs to reconsider the possibility of ductilizing RHEAs that are intrinsically brittle at RT but strong at HT. Here, an original strategy employing solid solution softening (SSS) at RT and solid solution hardening (SSH) at elevated temperatures was developed for single phase bcc-structured RHEAs, which greatly reduced the temperature dependence of yield stress (not monotonically reducing strength with increasing temperature) in this type of materials and helped to strike a better balance between RT ductility and HT strength. SSS is a well-established strategy to ductilize single phase bcc-structured refractory materials such as Mo and W based alloys, exemplified by the Re effect [8, 9]. Our previous work [10] also showed that Mn and Al are effective softeners in RHEAs, causing around 20% hardness reduction at RT in a ductile $Hf_{20}Nb_{31}Ta_{31}Ti_{18}$ RHEA; however, due to the limited SSH, the hardness exhibited an undesirable overall softening at the intermediate temperature range. Here in this work, Mn, as the solo alloying element, was added to a base $(HfNbTi)_{85}Mo_{15}$ RHEA, which is brittle at RT, to testify whether SSS is also valid in this situation. More importantly, it was intended to testify whether SSH, as the most common strengthening mechanism [11–13], can achieve an overall hardening at the intermediate temperature range.

Methods

RHEAs with nominal compositions of $(HfNbTi)_{85-x}Mo_{15}Mn_x$ (x = 2, 1, 0.3, 0.1, 0.03, 0 at%, with alloys denoted as Mn2, Mn1, Mn0.3, Mn0.1, Mn0.03, the base alloy, respectively) were produced by arc melting of high purity (>99.95%) elements at least 5 times to ensure chemical homogeneity followed by furnace cooling. Microstructure and chemical compositions were examined by field emission gun scanning electron microscope (FEGSEM, LEO-1550) equipped with backscatter electron (BSE) detector and energy dispersive spectroscopy (EDS). Seen from table 1, there was significant loss of Mn during melting, due to its low melting points compared to those of refractory elements and therefore its high volatilization, and a long melting time (>2 min per melting) at over 450 mA of arc melting current. The content of Mn was not able to be measured reliably with SEM-EDS. Instead, induction coupled plasma optical emission spectrometer (ICP-OES, Spectro Arcos) was used to measure the Mn content (in wt. %) and the results are given in table 1. The crystal structure was tested by x-ray diffractometer (XRD, Bruker D8 Advance), using Cu-$K_{\alpha 1}$ radiation in the 2theta range of 20° to 100°. Cylindrical specimens with a diameter of 6 mm and height of 9 mm were used for compressive tests. HT compressive experiments were carried out under high vacuum ($<4 \times 10^{-1}$ torr) on a Gleeble 3180 thermal-mechanical physical simulation system at 400 °C, 600 °C, 800 °C, and 1000 °C, respectively, with an initial strain rate of 10^{-3} s^{-1} and a maximum engineering strain of 60%. Each composition was tested 3 times at each temperature to guarantee the reproducibility of the results. A universal testing machine (Zwick Roll Z050) was used to measure the RT compressive yield stress in laboratory air with an initial strain rate of 10^{-3} s^{-1} and a maximum engineering strain around 25% due to the limitation of the load cell capacity. Two RT compression tests were done for each composition to guarantee the reproducibility of the results.

Results

Figure 1 shows the microstructures of the base alloy, Mn2, Mn1, Mn0.3, Mn0.1 and Mn0.03 alloys, where dendritic and inter-dendritic features typically seen in directly cast HEAs were observed. The average grain size of alloys studied here is around 100 um. An EDS elemental mapping of the base alloy, given in figure 2, shows the segregation of Mo and Nb with high T_m in the dendritic region, while Hf and Ti with relatively low T_m in the inter-dendritic region, and the similar patten was seen in all alloys tested here (not shown for simplicity). All tested alloys were identified to be of the single bcc phase according to figure 3, and no secondary phase was seen, which agrees with the SEM observations.

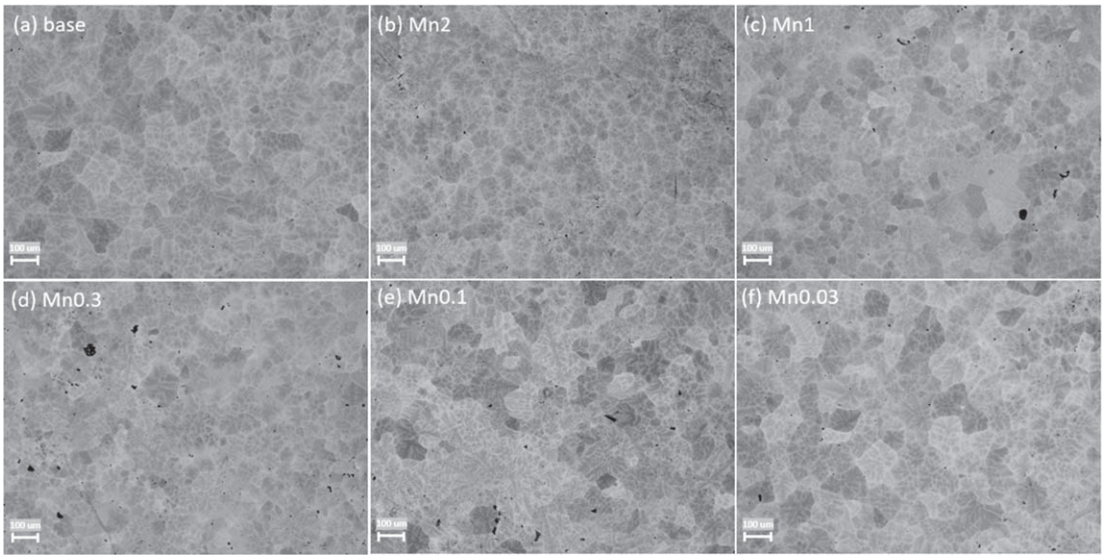

Figure 1. BSE images of (a) the base alloy, (b) Mn2, (c) Mn1, (d) Mn0.3, (e) Mn0.1 and (f) Mn0.03 alloys.

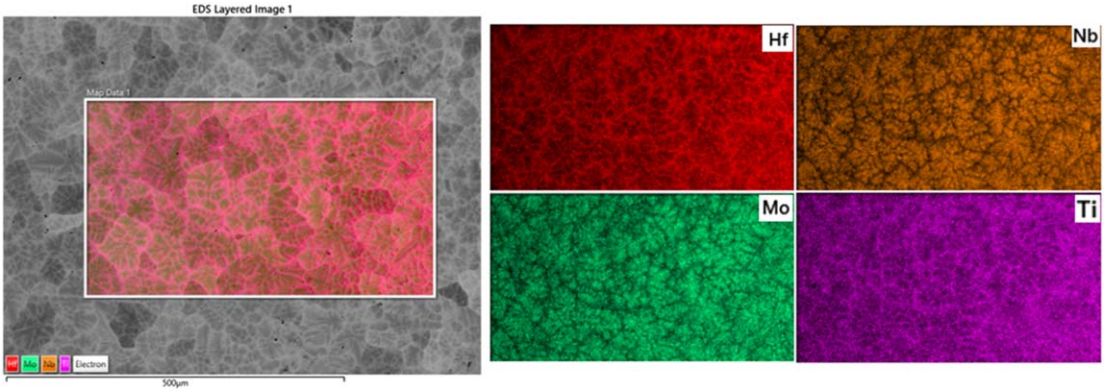

Figure 2. EDS elemental mappings of the base alloy.

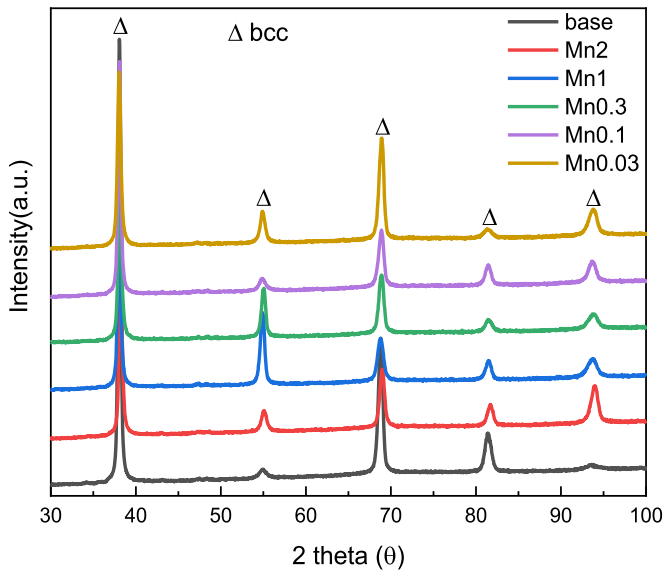

Figure 3. XRD patterns of the base alloy, Mn2, Mn1, Mn0.3, Mn0.1 and Mn0.03 alloys, respectively.

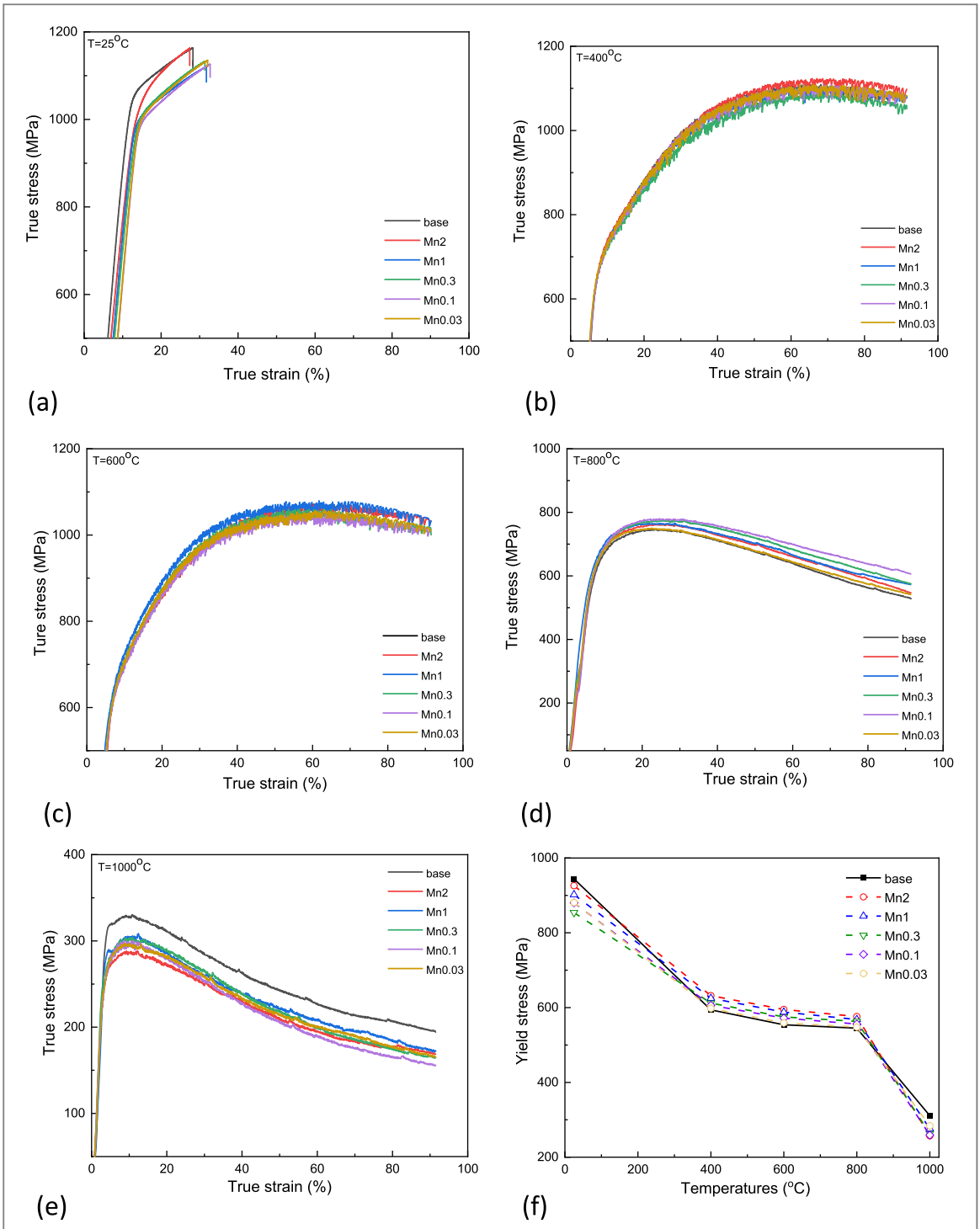

Figure 4. Compressive true strain-stress curves at (a) RT, (b) 400 °C, (c) 600 °C, (d) 800 °C, (e) 1000 °C for the base alloy, Mn2, Mn1, Mn0.3, Mn0.1, Mn0.03 alloys studied here. (f) Temperature dependence of compressive yield stress for all studied alloys from RT to 1000 °C.

Compressive true strain-stress curves for all studied alloys are shown in figures 4 (a)–(e). It is noted that all alloys studied here did not show any sign of fracture with the testing facility limitation on the maximum engineering strain. The compressive strain is therefore not discussed, and the peak stress at RT could unfortunately not be measured. As such, we focus more on the yield stresses of studied alloys, and their variation with compositions and temperatures. Nevertheless, measured yield stresses and peak stresses of studied alloys are summarized in table 2. For clarity, the temperature dependence of yield stress of all studied alloys from RT to 1000 °C is summarized in figure 4 (f). Some salient features are seen from both figure4(f) and table 2. Firstly, Mn additions indeed softened the base alloy at RT in all cases, with the maximum softening occurred at Mn0.3. This also nicely agreed with the hardness measurements, where the base alloy had the hardness of HV5 380 (±4), while Mn doped alloys had the hardness of HV5 358 (±6), 348 (±6), 341(±4), 350 (±3) and 342 (±4),

Table 2. Compression yield stress (σ_y), and peak stress (σ_p) of the studied alloys given in the form of σ_y/σ_p, at the temperature range from RT to 1000 °C.

Alloys /Temperatures(°C)	Base	Mn2	Mn1	Mn0.3	Mn0.1	Mn0.03
RT[1]	944/-	926/-	902/-	854/-	880/-	881/-
400 °C[2]	594/1101	632/1117	625/1099	612/1087	606/1095	598/1099
600 °C[2]	554/1015	595/1060	588/1076	575/1032	572/1047	559/1032
800 °C[2]	545/745	576/767	568/770	563/776	556/779	548/749
1000 °C[2]	311/328	257/288	276/305	263/303	259/296	254/295

1: tested using the universal compressive machine; 2: tested using the Gleeble system.

respectively, for Mn2, Mn1, Mn0.3, Mn0.1 and Mn0.03. Secondly, at the intermediate temperature range from 400 °C to 800 °C, Mn additions hardened the base alloy in all cases, and the hardening level (for yield strength) increased with increasing Mn content. The seen SSS at RT and SSH at elevated temperatures are exactly what we expected to achieve. Thirdly, SSS instead of SSH occurred at temperatures higher than 800 °C, where it was seen that the base alloy was stronger than all Mn doped alloys. Figure 4(f) also shows a typical three-stage pattern that is widely observed for the temperature-dependent yield stress in bcc-structured materials: at temperatures between RT and 400 °C, the yield stress showed the temperature dependence, known as the thermal effective stress [14], where the yield stress decreased with increasing temperature; at intermediate temperatures between 400 °C to 800 °C, a temperature independent yield stress was seen, known as the athermal stress. The barrier which gives rise to thermal effective stress is of a short-range nature and by contrast, the barrier which gives rise to athermal stress is of a long-range nature. Therefore, they (thermal effective stress and athermal stress) will have different interactions with dislocations upon alloying with solute additions [14], which will be discussed below; at temperatures above 800 °C, the yield stress decreased quickly.

Discussion

The yield stress of the base alloy was higher than those alloys with minor Mn additions, thus showing a SSS effect at RT. To be specific, nominal additions of 2%, 1%, 0.3%, 0.1%, 0.03% of Mn softened the base alloy by 2.0%, 4.4%, 9.5%, 6.8%, 6.7%, respectively, in terms of yield stress, which is 5.8%, 8.4%, 10.3%, 7.9%, 10.0%, respectively, in terms of hardness. The softening is most significant at nominal addition of 0.3% Mn. Seen from figure 4(f), at the temperature range from RT to 400 °C, the yield stress showed a strong temperature dependence. It is well known that the plastic deformation of bcc-structured metallic materials is mediated by the motion of $1/2\langle 111\rangle$ screw dislocations with a non-planar core and their interactions with solutes. The double-kink nucleation process would occur spontaneously due to the lowest Gibbs free energy configuration [15, 16]. The double-kink nucleation accommodates screw dislocations and hence induces softening, only at low temperatures. On the other hand, the kink migration process moving laterally along the dislocation line pushes the screw dislocations forward, and it leads to hardening, which is possible at the whole temperature range. These two competing mechanisms, double-kink nucleation and kink migration are both thermally activated, and their rates can be described by the Arrhenius equation as (attempt frequency) * exp [-(enthalpy barrier)/(k_BT)], where k_B is Boltzmann's constant and T is temperature [9]. The enthalpy barrier has an energy scale and a stress scale: the energy scale is connected to the direct solute-dislocation core interaction, while the stress scale is correlated to the Peierls misfit (the ability to change stiffness) for moving a single atomic row in the dislocation core, which is sensitive to the local chemical environment [8]. To induce ductility by softening at low temperatures, the double-kink nucleation mechanism shall dominate the plastic deformation behavior rather than the kink migration mechanism. In principle, under a certain critical amount, any type of solute additions shall lead to double-kink nucleation, no matter their interactions with screw dislocations are attractive or repulsive. With a less than 2 at. % nominal addition of Mn into the base alloy, presumably it caused attractive interactions with screw dislocations and a decreased stiffness of the dislocation core because of a higher d electron number of Mn compared to the alloying elements in the base alloy [9, 17]. Thus, the double-kink nucleation process initiated first and dominated the plastic deformation behavior unless with more alloying additions the massive kink migration eventually would lead to an overall hardening effect. Also, seen from figure 4(f), when the nominal addition of Mn decreased from 2 at. % to 0.03 at. %, the softening maximized at 0.3 at% addition. Supposedly, there is an ideal concentration for softening and this ideal concentration varies with type of solutes and temperature, around 0.3 at. % for Mn at RT here in this case. Due to the short-range nature of the (double) kink nucleation energy barrier between local solutes and dislocations [17, 18], a generic theoretic prediction for effective stress, the thermal component of flow stress in bcc structured materials, is not easy. Therefore, it is challenging to theoretically predict the alloying addition for maximized softening.

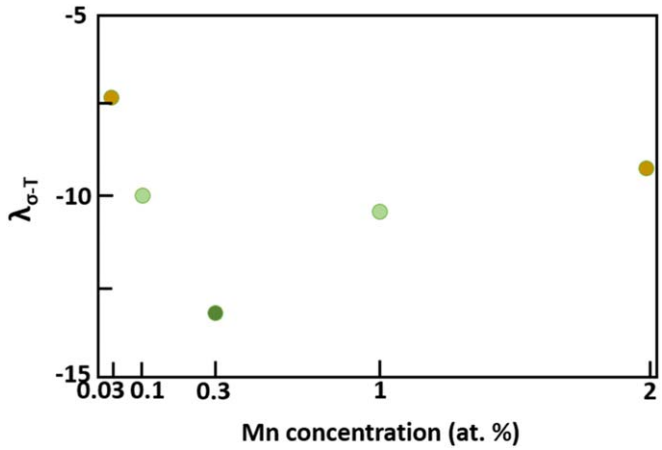

Figure 5. Variation of the temperature dependence descriptor of the yield stress, $\lambda_{\sigma-T,}$ for alloys with different Mn additions.

At the intermediate temperature, from 400 °C to 800 °C in this case, the yield stress was almost stabilized. Also, the yield stress of the base alloy was lower than those with minor Mn additions, thus displaying a SSH effect. Taking the yield stress measured at 600 °C as an example, the nominal addition of 2%, 1%, 0.3%, 0.1%, 0.03% of Mn hardened the base alloy by 7.4%, 6.1%, 3.8%, 3.2%, 0.9%, respectively. The hardening level decreased with decreasing Mn content. With a significant thermal aiding at elevated temperatures, dislocations spread under different modes such as lateral kink migration, and Peierls advancement and cross-kink gliding are dominating at the intermediate temperature range. It is widely accepted that SSH in metallic materials results from the elastic stress field interactions between solute atoms and dislocations [12, 19]. The addition of solutes induces a stress increase, $\Delta\sigma$, which can be expressed as $\Delta\sigma = A\mu\delta^{4/3}\, c^{2/3}$ [20, 21]. Here, A is a material-dependent dimensionless constant, μ is the shear modulus of the alloy, c is the solute atom concentration, and δ is the lattice misfit parameter including atomic size and modulus differences among constituent alloying elements. Thus, in principle a direct correlation between the stress increase (i.e., hardening) and lattice misfit parameter can be established for a single-phase solid solution. A rough landscape with lattice distortion caused by atomic size and modulus misfit is shielded for dislocations to move across. Mn has a relatively smaller atomic radius (135 pm) compared to that of Ti (146 pm), Hf (158 pm), Nb (143 pm), therefore, the reducing nominal addition of Mn from 2 at. % down to 0.03 at. % caused a reduced lattice distortion and hence reduced hardening in the base alloy. The hardening was small but importantly it caused an overall hardening effect at the intermediate temperature range, which significantly differentiated from the case in our previous work where a nominal addition of 2.5at% of Mn, Al, and Cu softened the base $Hf_{20}Nb_{31}Ta_{31}Ti_{18}$ alloy at both RT and the intermediate temperature range [10].

A temperature dependence descriptor of yield stress applicable to the low and intermediate temperature range is defined here as: $\lambda_{\sigma-T} = a-b$. Here a is the yield stress difference (percentage) at RT, while b is the yield stress difference (percentage) at the intermediate temperature range, both relative to the base alloy. We assign the yield stress difference negative value for the softening case, and positive value for the hardening case. A lower $\lambda_{\sigma-T}$ represents a lower temperature dependence of the yield stress before reaching HT, so from RT spanning the intermediate temperature range, which is a desirable scenario that one attempts to achieve for potential HT materials. This temperature dependence descriptor of yield stress can indirectly represent the structural and thermal stability of alloys and can be used to evaluate the reliability of potential HT alloys under service conditions. Again, taking 600 °C as an example, $\lambda_{\sigma-T}$ for the alloys with nominal 2%, 1%, 0.3%, 0.1%, 0.03% of Mn additions are $(-2.0–7.4) = -9.4$, $(-4.4–6.1) = -10.5$, $(-9.5–3.8) = -13.3$, $(-6.8–3.2) = -10.0$, $(-6.7–0.9) = -7.6$, respectively (see figure 5). $\lambda_{\sigma-T}$ for the Mn0.3 alloy is the lowest among all alloys up to 800 °C, meaning a better balance between SSS at low temperatures and SSH at the intermediate temperature range.

At high temperatures, 1000 °C in this case, the yield stress experienced a quick drop regardless of the amount of Mn additions, due to a typical softening mechanism associated with the activation of thermal diffusional processes and the low melting point of Mn thus its fast diffusion. The plastic deformation at this high temperature range is more studied for time-dependent mechanical properties such as creep and fatigue, which is beyond the scope of the current work.

Conclusion

In summary, better balanced strength from low temperatures to intermediate temperatures in a $(TiHfNb)_{85}Mo_{15}$ RHEA was experimentally achieved here by less than 2 at. % nominal additions of Mn, combining strategies of SSS at low temperatures and SSH at intermediate temperatures. The yield stress of all studied alloys showed a three-stage pattern: a temperature dependent state at low temperatures governed by SSS, an athermal stage at intermediate temperatures controlled by SSH, and another temperature dependent stage at high temperatures influenced by enhanced thermal diffusional processes. The alloy with 0.3 at. % Mn addition showed the largest softening effect by 9.5% at RT. The same alloy also exhibited the lowest temperature dependence descriptor $\lambda_{\sigma-T}$ among all studied alloys, indicating the lowest temperature dependence of yield stress before reaching the high temperature range. Overall, SSS at low temperatures holds the potential to induce non-zero tensile ductility for those RHEAs with decent HT strength, which would alleviate the manufacturing and processing concerns, while a simultaneous improvement of yield stress at intermediate temperatures by SSH is important for their applications at elevated temperatures.

Acknowledgments

XL and SG thank the financial support from the Swedish Research Council (grant number 2019–03559). XL is also grateful for the financial support from the Axel Hultgrens Fund. QH thanks the financial support from Department of Science and Technology of Jiangxi Province, China (grant number 20232BBH80008).

Data availability statement

All data that support the findings of this study are included within the article (and any supplementary files).

ORCID iDs

Sheng Guo https://orcid.org/0000-0001-8349-3135

References

[1] Senkov O N, Wilks G B, Miracle D B, Chuang C P and Liaw P K 2010 *Intermetallics* **18** 1758–65
[2] Senkov O N, Wilks G B, Scott J M and Miracle D B 2011 *Intermetallics* **19** 698–706
[3] Senkov O N, Miracle D B and Rao S I 2021 *Mater. Sci. Eng. A* **820** 141512
[4] Guo S, Ng C, Lu J and Liu C T 2011 *J. Appl. Phys.* **109** 103505
[5] Sheikh S, Shafeie S, Hu Q, Ahlström J, Persson C, Veselý J, Zýka J, Klement U and Guo S 2016 *J. Appl. Phys.* **120** 164902
[6] Huang H *et al* 2017 *Adv. Mater.* **29** 1701678
[7] Senkov O N, Miracle D B, Chaput K J and Couzinie J P 2018 *J. Mater. Res.* **33** 3092–128
[8] Klopp W D 1968 Review of ductilizing of group VIA elements by rhenium and other solutes *National Aeronautics and Space Administration* 4955
[9] Trinkle D R and Woodward C 2005 *Science* **310** 1665–7
[10] Li X L, Lu J, Mao H H, Murakami H and Guo S 2023 *AIP Adv.* **13** 085033.
[11] Rao S I, Woodward C, Akdim B, Senkov O N and Miracle D 2021 *Acta Mater.* **209** 116758
[12] Suzuki T 1981 *Jpn. J. Appl. Phys.* **20** 449
[13] Sun Y, Chen P, Liu L, Yan M, Wu X, Yu C and Liu Z 2018 *Intermetallics* **93** 85–8
[14] Arsenault R J 1969 *Actaz. Metallurgica.* **17** 1291–7
[15] Ghafarollahi A and Curtin W A 2020 *Acta Mater.* **196** 635–50
[16] Maresca F and Curtin W A 2020 *Acta Mater.* **182** 144–62
[17] Hu Y J, Fellinger M R, Bulter B G, Wang Y, Darling K A, Kecskes L J, Trinkle D R and Liu Z K 2017 *Acta Mater.* **141** 304–16
[18] Coury F G 2018 Solid solution strengthening mechanisms in high entropy alloys *PhD thesis, Colorado School of Mines, Golden* p 86
[19] Gypen L A and Deruyttere A 1981 *Scr. Metallurgica.* **15** 815–20
[20] Labusch R 1970 *Phys. Stat. Sol.* **41** 659–69
[21] Senkov O N, Scott J M, Senkova S V, Miracle D B and Woodward cf 2011 *J. Alloys Compd.* **509** 6043–8